A COMPUTATIONAL APPROACH FOR THE INVERSE PROBLEM OF NEURAL CONDUCTANCES DETERMINATION:

SUPPLEMENTARY MATERIAL

JEMY A. MANDUJANO VALLE, ALEXANDRE L. MADUREIRA, ANTONIO LEITÃO

Abstract. This paper contains some supplementary material on [1]. In the introduction, we describe the inverse problem in the cable equation. Therefore, in Section 2 and 3, we solve the partial differential equations numerically. Finally, we display figures for the numerical examples, considering 5% of noise in measuring the membrane potential.

1. Introduction

In the passive cable model the membrane electrical potential $V : [0,T] \times [0,L] \to \mathbb{R}$ solves

$$
(1) \quad \begin{cases} C_M V_t = \dfrac{r_a}{2R} V_{xx} - G_L(V - E_L) - \displaystyle\sum_{i \in Ion} G_i(t,x)[V - E_i], & \text{in } (0,T) \times (0,L), \\ V(0,x) = r(x), & \text{in } x \in [0,L], \\ V_x(t,0) = p(t), \;\; V_x(t,L) = q(t), & \text{in } t \in [0,T]. \end{cases}
$$

where C_M represents membrane specific capacitance in microfarad per square centimeter ($\mu F/cm^2$); the potential V is in millivolt (mV); the time t is in milliseconds (ms); r_a is the radious of the fibre in millicentimeter (mcm); the specific resistance R is in ohm centimeter (Ωcm); the space x is in centimeter (cm); the constant leak specific conductance G_L is in millisiemens per square centimeter (mS/cm^2); E_L represents leak equilibrium potential in millivolt (mV); Ion is the set of ions of the model, e.g., Ion $= \{\mathrm{K}, \mathrm{Na}\}$. Also, the membrane specific conductance G_i for the ion $i \in$ Ion is in millisiemens per square centimeter (mS/cm^2), and it might depend on spatial and temporal variables, as indicated in the notation. Finally, the Nerst potential E_i for each ion $i \in$ Ion is given in millivolt (mV).

We assume that the constants C_M, r_a, R, G_L, E_L, E_i, T and L, and the functions p, q and r are given data. Let N_{ion} be the number of ions of the set Ion. For Ion $= \{1, 2, \cdots, N_{\text{ion}}\}$, $\boldsymbol{G}(t,x) = (G_1(t,x), \ldots, G_{N_{\text{ion}}}(t,x))$. We want to estimate $\boldsymbol{G}$, from differential equation (1), given measurements of the voltage.

Date: January 07, 2020.

We consider the nonlinear operator

$$F : D(F) \to R(F) \tag{2}$$

that associates for a given $\boldsymbol{G} \in D(F)$ the resulting voltage, i.e., $F(\boldsymbol{G}) = V|_\Gamma$, where $\Gamma = \{(t,x);\ \ 0 \le t \le T,\ \ 0 \le x \le L\}$ or $\Gamma = \{(t,x);\ \ 0 \le t \le T,\ \ x \in \{0, L\}\}$. Note that V solves Eq. (1).

We consider the inverse problem of finding an approximation for $\boldsymbol{G}$ given the noisy data $V^\delta|_\Gamma$, where

$$\|V - V^\delta\|_{L^2(\Gamma)} \le \delta, \tag{3}$$

for some known noise threshold $\delta > 0$. That makes sense since, in practice, the data $V|_\Gamma$ are never known exactly.

Given an initial guess $\boldsymbol{G}^{1,\delta}$, the minimal error approximation for $\boldsymbol{G}$ is defined by the sequence

$$\boldsymbol{G}^{k+1,\delta} = \boldsymbol{G}^{k,\delta} + w^{k,\delta} F'(\boldsymbol{G}^{k,\delta})^*(V^\delta|_\Gamma - F(\boldsymbol{G}^{k,\delta})), \tag{4}$$

for $k = 1, 2, \ldots$, where $F'(\cdot)^*$ is adjoint of the Gâteux derivative, and

$$w^{k,\delta} = \frac{\|V^\delta - F(\boldsymbol{G}^{k,\delta})\|^2_{L^2(\Gamma)}}{\|F'(\boldsymbol{G}^{k,\delta})^* \left(V^\delta - F(\boldsymbol{G}^{k,\delta})\right)\|^2_{D(F)}}. \tag{5}$$

Iteration (4) stops at the minimum k_*, for a given $\tau > 2$, such that

$$\|V^\delta - F(\boldsymbol{G}^{k_*,\delta})\|_{L^2(\Gamma)} \le \tau\delta \le \|V^\delta - F(\boldsymbol{G}^{k,\delta})\|_{L^2(\Gamma)}. \tag{6}$$

From Eqs. (4) and (6) we obtain an approximation $\boldsymbol{G}^{k_*,\delta}$ for $\boldsymbol{G}$. Although the adjoint $F'(\boldsymbol{G}^{k,\delta})^*$ is not known, it is possible to show that Eq. (4) is actually

$$G_i^{k+1,\delta}(t,x) = G_i^{k,\delta}(t,x) - w^{k,\delta}(V^{k,\delta}(t,x) - E_i)U^k(t,x) \quad \text{for all } i \in \text{Ion}, \tag{7}$$

where

$$w^{k,\delta} = \frac{\|V^\delta - F(\boldsymbol{G}^{k,\delta})\|^2_{L^2(\Gamma)}}{\displaystyle\sum_{i\in\text{Ion}} \left\| \left(V^{k,\delta}(t,x) - E_i\right) U^k(t,x)\right\|^2_{D(F)}}.$$

Also, $V^{k,\delta}$ solves Eq. (1) with $\boldsymbol{G}$ replaced by $\boldsymbol{G}^{k,\delta}$, and U^k solves the Eq. (8) replacing V by $V^{k,\delta}$ and G_i by $G_i^{k,\delta}$.

$$
\begin{cases}
-\dfrac{r_a}{2R}U_{xx} - C_M U_t + G_L U + \displaystyle\sum_{i\in \mathrm{Ion}} G_i(t,x)U = \alpha_1\left(V^\delta - V\right), & \text{in } (0,T)\times(0,L),\\
U(T,x) = 0, & \text{in } x\in[0,L],\\
U_x(t,0) = -\alpha_2\dfrac{2R}{r_a}\left(V^\delta(t,0) - V(t,0)\right), & \text{in } t\in[0,T],\\
U_x(t,L) = \alpha_2\dfrac{2R}{r_a}\left(V^\delta(t,L) - V(t,L)\right), & \text{in } t\in[0,T].
\end{cases} \tag{8}
$$

The numerical scheme of our method is as follows. Note from Algorithm 1 that solutions of two PDEs are needed for each iteration.

Data: $V^\delta|_\Gamma$, r, p, q, δ, τ

Result: Compute an approximation for $\boldsymbol{G}$ using minimal error Iteration Scheme

Choose $\boldsymbol{G}^{1,\delta}$ as an initial approximation for $\boldsymbol{G}$;

Compute $V^{1,\delta}$ from Eq. (1), replacing $\boldsymbol{G}$ by $\boldsymbol{G}^{1,\delta}$;

k=1;

while $\tau\delta \le \|V^\delta - V^{k,\delta}\|_{L^2(\Gamma)}$ **do**

  Compute U^k from Eq. (8), replacing V by $V^{k,\delta}$ and G_i by $G_i^{k,\delta}$;

  Compute $\boldsymbol{G}^{k+1,\delta}$ using Eq. (7);

  Compute $V^{k+1,\delta}$ from Eq. (1), replacing $\boldsymbol{G}$ by $\boldsymbol{G}^{k+1,\delta}$;

  $k \leftarrow k+1$;

end

Algorithm 1: Minimal Error Iteration

1.1. **The minimal error method applied to the conductance determination defined on a branched tree.** Following Figure 1, we let $\Theta = \mathcal{E}\cup\mathcal{V}$ be a branched tree, where $\mathcal{E} = \{e_1, e_2, e_3\}$ is a set of edges, $\mathcal{V} = \{\nu_1, \nu_2, \nu_3, \nu_4\}$ is a set of vertices, and the edges are connected at the vertices ν_j.

Our cable equation model defined on a branched tree is given by

$$
\begin{cases}
C_M V_t = \dfrac{r_a}{2R}V_{xx} - G_L(V - E_L) - \displaystyle\sum_{i\in Ion} G_i(t,x)\left[V - E_i\right], & \text{in } (0,T)\times\mathcal{E},\\
V(0,x) = r(x), & \text{in } x\in\Theta,\\
V_x(t,\gamma_1) = p(t), & \text{in } t\in[0,T],\\
V_x(t,\gamma_2) = V_x(t,\gamma_3) = q(t), & \text{in } t\in[0,T],\\
V_x^{e_1}(t,\nu_2) - V_x^{e_2}(t,\nu_2) - V_x^{e_3}(t,\nu_2) = 0, & \text{in } t\in[0,T],
\end{cases} \tag{9}
$$

where $V_x^{e_j}(t,\nu_2)$ denotes the derivative of V at the vertex ν_2 taken along the edge $e_j \in \{e_1, e_2, e_3\}$ in the direction towards the vertex.

Consider operator (2) with $x \in \Theta$, such that $F(\boldsymbol{G}) = V(\cdot,\cdot)$, where V solves Eq. (9). The objective of this section, given V^δ, is to obtain an approximation to $\boldsymbol{G}$, using the method Eq. (4). To compute the adjoint operator $F^{'}(\cdot)^*$, we define, replacing U by $U^{k,\delta}$, V by $V^{k,\delta}$ and G_i by $G_i^{k,\delta}$, the following PDE:

$$
\begin{cases}
-\dfrac{r_a}{2R}U_{xx} - C_M U_t + G_L U + \displaystyle\sum_{i\in Ion} G_i(t,x)U = V^\delta - V, & \text{in } (0,T)\times\mathcal{E},\\
U(T,x) = 0, & \text{in } x \in \Theta,\\
U_x(t,0) = U_x^k(t,\nu_2) = U_x^k(t,\nu_3) = 0, & \text{in } t \in [0,T],\\
U_x^{e_1}(t,\nu_1) - U_x^{e_2}(t,\nu_1) - U_x^{e_3}(t,\nu_1) = 0, & \text{in } t \in [0,T].
\end{cases} \tag{10}
$$

We then compute $G_i^{k+1,\delta}$ according to (7).

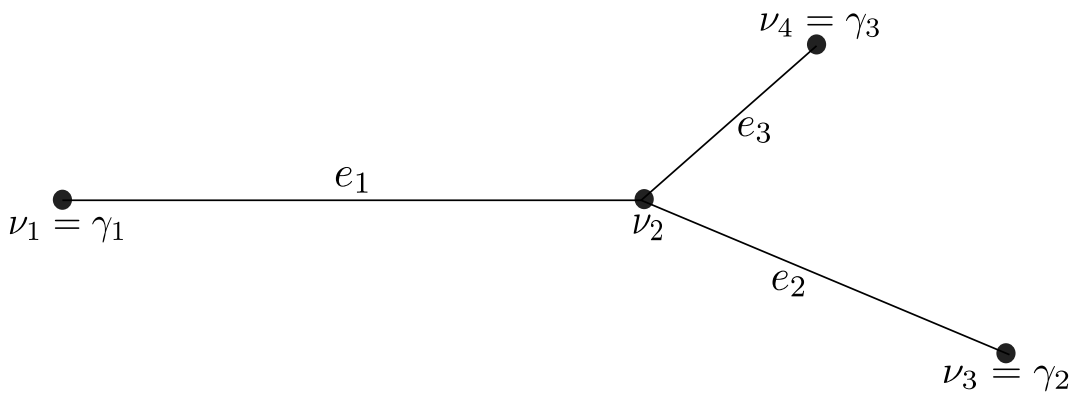

FIGURE 1. Example of a branched tree with one bifurcation point.

2. The backward Euler method for numerical solution of the cable equation

Dividing the interval $[0, L]$, of the spatial variable x, into "$J-1$" equal parts of length Δx, we have the "J" points $x_j = j\Delta x$, $j = 1, 2, \cdots, J$, where $\Delta x = L/(J-1)$ and, dividing the interval $[0, T]$, of the time variable t, in "$N-1$" equal parts in length Δt, we have the "N" points $t_n = n\Delta t$, $n = 1, 2, \cdots, N$, where $\Delta t = T/(N-1)$. So we will get an approximation of the solution at the points (t_n, x_j) of the mesh.

2.1. **Cable equation with initial condition.** Applying regressive differences on the right side of equation (1) and centralized differences on the left side, we have the following equation of order $O(\Delta t, \Delta x^2)$:

$$C_M \frac{V_j^{n+1} - V_j^n}{\Delta t} = \frac{r_a}{2R} \frac{V_{j-1}^{n+1} - 2V_j^{n+1} + V_{j-1}^{n+1}}{\Delta x^2} - G_L(V_j^{n+1} - E_L) - \sum_{i \in \text{Ion}} G_{ij}^{n+1} \left(V_j^{n+1} - E_i\right),$$

then

$$V_j^{n+1} - V_j^n = \frac{\Delta t\ r_a}{C_M 2R\Delta x^2} \left(V_{j-1}^{n+1} - 2V_j^{n+1} + V_{j-1}^{n+1}\right) - \frac{\Delta t}{C_M} G_L \left(V_j^{n+1} - E_L\right) - \frac{\Delta t}{C_M} \sum_{i \in \text{Ion}} G_{ij}^{n+1} \left(V_j^{n+1} - E_i\right),$$

we denote

$$a = \frac{\Delta t\ r_a}{C_M 2R\Delta x^2}, \qquad b_j^{n+1} = 1 + 2a + \frac{\Delta t}{C_M} G_L + \frac{\Delta t}{C_M} \sum_{i \in Ion} G_{ij}^{n+1}$$

and

$$c_j^{n+1} = \frac{\Delta t}{C_M} G_L E_L + \frac{\Delta t}{C_M} \sum_{i \in Ion} G_{ij}^{n+1} E_i.$$

Therefore

$$V_j^n = -aV_{j-1}^{n+1} + b_j^{n+1} V_j^{n+1} - aV_{j+1}^{n+1} + c_j^{n+1}. \tag{11}$$

Discretizing the Neumann boundary condition,

$$\frac{V_1^n - V_0^n}{\Delta x} = p^n \qquad \text{and} \qquad \frac{V_{J+1}^n - V_J^n}{\Delta x} = q^n,$$

then

$$V_0^n = V_1^n - \Delta x p^n \qquad \text{and} \qquad V_{J+1}^n = V_J^n + \Delta x q^n. \tag{12}$$

From equations (11) and (12), we have the following system of equations

$$\begin{aligned}
V_1^n &= \left(b_1^{n+1} - a\right) V_1^{n+1} - aV_2^{n+1} + 0V_3^{n+1} + c_1^{n+1} + a\Delta x p^{n+1} \\
V_j^n &= -aV_{j-1}^{n+1} + b_j^{n+1} V_j^{n+1} - aV_{j+1}^{n+1} + c_j^{n+1} \\
V_J^n &= 0V_{J-2}^{n+1} - aV_{J-1}^{n+1} + \left(b_J^{n+1} - a\right) V_J^{n+1} + c_J^{n+1} - a\Delta x q^{n+1}.
\end{aligned}$$

We introduce matrices

$$A^n = \begin{bmatrix} b_1^n - a & -a & 0 & \dots & 0 & 0 & 0 \\ -a & b_2^n & -a & \dots & 0 & 0 & 0 \\ 0 & -a & b_3^n & \dots & 0 & 0 & 0 \\ \vdots & \vdots & \vdots & \ddots & \vdots & \vdots & \vdots \\ 0 & 0 & 0 & \cdots & b_{J-2}^n & -a & 0 \\ 0 & 0 & 0 & \cdots & -a & b_{J-1}^n & -a \\ 0 & 0 & 0 & \dots & 0 & -a & b_J^n - a \end{bmatrix}, \quad B^n = \begin{bmatrix} c_1^n + a\Delta x p^n \\ c_2^n \\ c_3^n \\ \vdots \\ c_{J-2}^n \\ c_{J-1}^n \\ c_J^n - a\Delta x q^n \end{bmatrix}.$$

We denote the transpose and inverse matrix of A by A^T and A^{-1}, respectively. Let matrix $V^n = [V_1^n \quad V_2^n \quad \cdots \quad V_J^n]^T$. Then, we obtain the following equation $V^{n+1} = (V^n - B^{n+1})\,(A^{n+1})^{-1}$ for $n = 1, 2, \cdots, N-1$, with initial condition $V_j^1 = r_j$ for $j = 1, 2, \cdots, J$.

2.2. **Cable equation with final condition.** Applying regressive differences on the right side of equation (8) and centralized differences on the left side, we have the following equation of order $O(\Delta t, \Delta x^2)$:

$$-\frac{r_a}{2R}\frac{U_{j-1}^n - 2U_j^n + U_{j+1}^n}{\Delta x^2} - C_M\frac{U_j^{n+1} - U_j^n}{\Delta t} + G_L U_j^n + \sum_{i\in \text{Ion}} G_{ij}^n U_j^n = \alpha_1\left(V_j^{\delta^n} - V_j^n\right),$$

then

$$-\frac{\Delta t\, r_a}{C_M 2R\Delta x^2}\left(U_{j-1}^n - 2U_j^n + U_{j+1}^n\right) - U_j^{n+1} + U_j^n + \frac{\Delta t}{C_M}G_L U_j^n + \frac{\Delta t}{C_M}\sum_{i\in \text{Ion}} G_{ij}^n U_j^n = \frac{\Delta t}{C_M}\alpha_1\left(V_j^{\delta^n} - V_j^n\right),$$

we denote

$$d_j^n = V_j^{\delta^n} - V_j^n, \quad e_j^n = \frac{\Delta t}{C_M}\alpha_1 d_j^n, \quad f_1^n = \Delta x \alpha_2 \frac{2R}{r_a} d_1^n, \quad \text{and} \quad f_J^n = \Delta x \alpha_3 \frac{2R}{r_a} d_J^n.$$

Therefore

$$U_j^{n+1} = -aU_{j-1}^n + b_j^n U_j^n - aU_{j+1}^n - e_j^n. \tag{13}$$

Discretizing the Neumann boundary condition,

$$\frac{U_1^n - U_0^n}{\Delta x} = \alpha_2\frac{2R}{r_a}\left(V_1^{\delta^n} - V_1^n\right) \qquad \text{and} \qquad \frac{U_{J+1}^n - U_J^n}{\Delta x} = \alpha_3\frac{2R}{r_a}\left(V_J^{\delta^n} - V_J^n\right),$$

then

$$U_0^n = U_1^n - f_1^n \quad \text{and} \quad U_{J+1}^{n+1} = U_J^{n+1} + f_J^n. \tag{14}$$

From equations (13) and (14), we have the following system of equations

$$\begin{array}{rcrcrcrcl} U_1^{n+1} & = & (b_1^n - a)\, U_1^{n+1} & - & aU_2^n & + & 0U_3^n & - & (e_1^n - f^n) \\ U_j^{n+1} & = & -aU_{j-1}^n & + & b_j^n U_j^n & - & aU_{j+1}^n & - & \left(e_j^n - 0\ \right) \\ U_J^{n+1} & = & 0U_{J-2}^n & - & aU_{J-1}^n & + & (b_J^n - a)\, U_J^n & - & (e_J^n + f_J^n) \end{array}$$

We write the matrix $C^n = \begin{bmatrix} e_1^n - f_1^n & e_2^n & e_3^n & \cdots & e_{J-1}^n & e_J^n + f_J^n \end{bmatrix}^T$. Then, from system of equations, we obtain $U^n = (A^n)^{-1}\,(U^{n+1} + C^n)$ for $n = N-1, N-2, \cdots, 1$, with final condition $U_j^N = 0$ for $j = 1, 2, \cdots, J$.

3. The forward Euler method for numerical solution of the cable equation defined on a tree graph

The discretization of the temporal domain [0, T] is represented by a finite number of mesh points $0 = t_1 < t_2 < \cdots < t_N = T$. Dividing the edges $[\nu_1, \nu_2]$, $(\nu_2, \nu_3]$ and $[\nu_2, \nu_4]$, of the spatial variable in x, into $J_2 - 2$ equal parts of length Δx. Interval $[\nu_1, \nu_2]$ has "J" points $x_j = j\Delta x$, $j = 1, 2, \cdots, J$. Interval $(\nu_2, \nu_3]$ has "$J_1 - J$" points $x_j = j\Delta x$, $j = J+1, J+2, \cdots, J_1$. Finally, interval $[\nu_2, \nu_4]$ has "$J_2 - J_1$" points $x_j = j\Delta x$, $j = J_1 + 1, J_1 + 2, \cdots, J_2$, see Figure 2

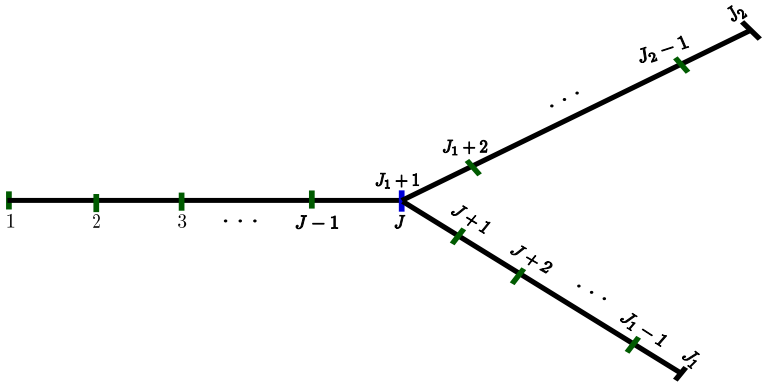

FIGURE 2. Spatial discretization.

3.1. **Cable equation with initial condition.** Applying finite differences in the first equation from (9), we obtain

$$\begin{aligned} C_M V_t &= \frac{r_a}{2R} V_{xx} - G_L(V - E_L) - \sum_{i \in \text{Ion}} G_i(t,x)\,[V - E_K]\,, \\ C_M \frac{V_j^{n+1} - V_j^n}{\Delta t} &= \frac{r_a}{2R} \frac{V_{j-1}^n - 2V_j^n + V_{j-1}^n}{\Delta x^2} - G_L(V_j^n - E_L) - \sum_{i \in \text{Ion}} G_{i\,j}^n \left(V_j^n - E_K\right), \\ V_j^{n+1} - V_j^n &= \frac{\Delta t\; r_a}{C_M 2R \Delta x^2} \left(V_{j-1}^n - 2V_j^n + V_{j+1}^n\right) - \frac{\Delta t}{C_M} G_L \left(V_j^n - E_L\right) \\ &\qquad - \frac{\Delta t}{C_M} \sum_{i \in \text{Ion}} G_{i\,j}^n \left(V_j^n - E_K\right). \end{aligned}$$

We denote

$$a = \frac{\Delta t\; r_a}{C_M 2R \Delta x^2}, \quad b_j^n = 1 - 2a - \frac{\Delta t}{C_M} G_L - \frac{\Delta t}{C_M} \sum_{i \in \text{Ion}} G_{i\,j}^n \quad \text{and} \quad c_j^n = \frac{\Delta t}{C_M} G_L E_L + \frac{\Delta t}{C_M} \sum_{i \in \text{Ion}} G_{i\,j}^n E_K$$

Therefore

$$V_j^{n+1} = a V_{j-1}^n + b_j^n V_j^n + a V_{j+1}^n + c_j^n, \tag{15}$$

Discretizing the Neumann boundary condition

$$\frac{V_1^n - V_0^n}{\Delta x} = p^n, \quad \frac{V_{J_1+1}^n - V_{J_1}^n}{\Delta x} = q^n \quad \text{and} \quad \frac{V_{J_2+1}^n - V_{J_2}^n}{\Delta x} = q^n,$$

then

$$V_0^n = V_1^n - \Delta x p^n, \quad V_{J_1+1}^n = V_{J_1}^n + \Delta x q^n \quad \text{and} \quad V_{J_2+1}^n = V_{J_2}^n + \Delta x q^n. \tag{16}$$

Discretizing the bifurcation point, in this case, we have two possibilities,

$$\frac{{V^{e_1}}_J^n - {V^{e_1}}_{J-1}^n}{\Delta x} - \frac{{V^{e_2}}_{J+1}^n - {V^{e_2}}_J^n}{\Delta x} - \frac{{V^{e_3}}_{J_1+1}^n - {V^{e_3}}_{J_1}^n}{\Delta x} = 0,$$

or

$$\frac{{V^{e_1}}_{J+1}^n - {V^{e_1}}_J^n}{\Delta x} - \frac{{V^{e_2}}_{J+1}^n - {V^{e_2}}_J^n}{\Delta x} - \frac{{V^{e_3}}_{J_1+1}^n - {V^{e_3}}_{J_1}^n}{\Delta x} = 0,$$

Note that ${V^{e_1}}_J^n = {V^{e_2}}_J^n$ and ${V^{e_1}}_{J+1}^n = {V^{e_2}}_{J+1}^n$. Then

$$V_{J_1}^n = V_{J-1}^n - 2V_J^n + V_{J+1}^n + V_{J_1+1}^n \quad \text{or} \quad V_{J_1}^n = V_{J_1+1}^n, \tag{17}$$

here, we consider $V_{J_1}^n = V_{J_1+1}^n$.

From equations (15) , (16) and (17), we have the following system of equations

$$\begin{aligned}
V_1^{n+1} &= (b_1^n + a)\, V_1^n + aV_2^n + 0V_3^n + c_1^n - a\Delta x p^n \\
V_j^{n+1} &= aV_{j-1}^n + b_j^n V_j^n + aV_{j+1}^n + c_j^n \\
V_{J_1}^{n+1} &= aV_{J_1-1}^n + \left(b_{J_1}^n + a\right) V_{J_1}^n + 0V_{J_1+1}^n + c_{J_1}^n + a\Delta x q^n \\
V_{J_1+1}^{n+1} &= 0V_{J_1}^n + \left(b_{J_1+1}^n + a\right) V_{J_1+1}^n + aV_{J_1+2}^n + c_{J_1+1}^n \\
V_j^{n+1} &= aV_{j-1}^n + b_j^n V_j^n + aV_{j+1}^n + c_j^n \\
V_{J_2}^{n+1} &= aV_{J_2-1}^n + (a + b_{J_2})\, V_{J_2}^n + 0V_{J_2+1}^n + c_{J_2}^n + a\Delta x q^n.
\end{aligned}$$

We introduce matrix

$$A^n = \begin{bmatrix}
a+b_1^n & a & 0 & 0 & 0 & & & \cdots & & & & 0 \\
a & b_2^n & a & 0 & 0 & & & \cdots & & & & 0 \\
\vdots & \ddots & \ddots & \ddots & \vdots & & & \vdots & & & & \vdots \\
0 & \cdots & 0 & a & b_{J_1-1}^n & a & 0 & 0 & 0 & 0 & \cdots & 0 \\
0 & \cdots & 0 & 0 & a & a+b_{J_1}^n & 0 & 0 & 0 & 0 & \cdots & 0 \\
0 & \cdots & 0 & 0 & 0 & 0 & a+b_{J_1+1} & a & 0 & 0 & \cdots & 0 \\
0 & \cdots & 0 & 0 & 0 & 0 & a & a+b_{J_1+2} & a & 0 & \cdots & 0 \\
\vdots & \vdots & \vdots & \vdots & \vdots & \vdots & \vdots & \ddots & \ddots & \ddots & \cdots & \vdots \\
0 & & & & & \cdots & & & 0 & a & b_{J_2-1}^n & a \\
0 & & & & & \cdots & & & 0 & 0 & a & a+b_{J_2}^n
\end{bmatrix}$$

and $B^n = \left[c_1^n - a\Delta p^n \quad c_2^n \quad \cdots \quad c_{J_1-1}^n \quad c_{J_1}^n + a\Delta x q^n \quad c_{J_1+1}^n \quad \cdots \quad c_{J_2-1}^n \quad c_{J_2}^n + a\Delta x q^n\right]^T$. Then, we obtain the following equation $V^{n+1} = A^n V^n + B^n$ for $n = 1, 2, \cdots, N-1$, with initial condition $V_j^1 = r_j$ for $j = 1, 2, \cdots, J$.

3.2. **Cable equation with final condition.** Applying finite differences in the first equation from (10), we obtain

$$\begin{aligned}
-\frac{r_a}{2R} U_{xx} - C_M U_t + G_L U + \sum_{i \in \text{Ion}} G_i(t,x) U &= V^\delta - V, \\
-\frac{r_a}{2R} \frac{U_{j-1}^{n+1} - 2U_j^{n+1} + U_{j+1}^{n+1}}{\Delta x^2} - C_M \frac{U_j^{n+1} - U_j^n}{\Delta t} + G_L U_j^{n+1} + \sum_{i \in \text{Ion}} G_{ij}^{n+1} U_j^{n+1} &= V_j^{\delta^{n+1}} - V_j^{n+1},
\end{aligned}$$

then

$$-\frac{\Delta t\, r_a}{C_M 2R\Delta x^2}\left(U_{j-1}^{n+1}-2U_j^{n+1}+U_{j+1}^{n+1}\right)-\left(U_j^{n+1}-U_j^n\right)+\frac{\Delta t}{C_M}G_L U_j^{n+1} + \frac{\Delta t}{C_M}\sum_{i\in \text{Ion}} G_{ij}^{n+1}U_j^{n+1}=\frac{\Delta t}{C_M}\left(V_j^{\delta^{n+1}}-V_j^{n+1}\right).$$

We denote

$$d_j^{n+1}=\frac{\Delta t}{C_M}\left(V_j^{\delta^{n+1}}-V_j^{n+1}\right)$$

Therefore

$$U_j^n = aU_{j-1}^{n+1}+b_j^{n+1}U_j^{n+1}+aU_{j+1}^{n+1}+d_j^{n+1} \tag{18}$$

Discretizing the Neumann boundary condition,

$$\frac{U_1^n-U_0^n}{\Delta x}=\frac{U_{J_1+1}^n-U_{J_1}^n}{\Delta x}=\frac{U_{J_2+1}^n-U_{J_2}^n}{\Delta x}=0,$$

then

$$U_0^n=U_1^n,\quad U_{J_1+1}^n=U_{J_1}^n \quad \text{and} \quad U_{J_2+1}^n=U_{J_2}^n. \tag{19}$$

Discretizing the bifurcation point, in this case, also we have two possibilities,

$$\frac{U^{e_1 n}_{\ J}-U^{e_1 n}_{\ J-1}}{\Delta x}-\frac{U^{e_2 n}_{\ J+1}-U^{e_2 n}_{\ J}}{\Delta x}-\frac{U^{e_3 n}_{\ J_1+1}-U^{e_3 n}_{\ J_1}}{\Delta x}=0,$$

or

$$\frac{U^{e_1 n}_{\ J+1}-U^{e_1 n}_{\ J}}{\Delta x}-\frac{U^{e_2 n}_{\ J+1}-U^{e_2 n}_{\ J}}{\Delta x}-\frac{U^{e_3 n}_{\ J_1+1}-U^{e_3 n}_{\ J_1}}{\Delta x}=0$$

Note that $U^{e_1 n}_{\ J}=U^{e_2 n}_{\ J}$ and $U^{e_1 n}_{\ J+1}=U^{e_2 n}_{\ J+1}$. Then

$$U^{e_3 n}_{\ J_1}=U^{e_1 n}_{\ J-1}-2U^{e_2 n}_{\ J}+U^{e_2 n}_{\ J+1}+U^{e_3 n}_{\ J_1+1} \quad \text{or} \quad U^{e_3 n}_{\ J_1}=U^{e_3 n}_{\ J_1+1}, \tag{20}$$

here, we consider $U^{e_3 n}_{\ J_1}=U^{e_3 n}_{\ J_1+1}$.

From equation (18), (19) and (20), we have following system of equations

$$\begin{aligned}
U_1^n &= \left(b_1^{n+1}+a\right)U_1^{n+1} + aU_2^{n+1} + 0U_3^{n+1} + d_1^{n+1}\\
U_j^n &= aU_{j-1}^{n+1} + b_j^{n+1}U_j^{n+1} + aU_{j+1}^{n+1} + d_j^{n+1}\\
U_{J_1}^n &= aU_{J_1-1}^{n+1} + \left(b_{J_1}^{n+1}+a\right)U_{J_1}^{n+1} + 0U_{J_1+1}^{n+1} + d_{J_1}^{n+1}\\
U_{J_1+1}^n &= 0U_{J_1}^{n+1} + \left(b_{J_1+1}^{n+1}+a\right)U_{J_1+1}^{n+1} + aU_{J_1+2}^{n} + d_{J_1+1}^{n+1}\\
U_j^n &= aU_{j-1}^{n+1} + b_j^{n+1}U_j^{n+1} + aU_{j+1}^{n+1} + d_j^{n+1}\\
U_{J_2}^n &= aU_{J_2-1}^{n+1} + \left(a+b_{J_2}\right)U_{J_2}^{n+1} + 0U_{J_2+1}^{n+1} + d_{J_2}^{n+1}.
\end{aligned}$$

We denote matrix $D^n = [d_1^n \;\; d_2^n \;\; \cdots \;\; d_{J_2}^n]^T$ and $U^n = [U_1^n \;\; U_2^n \;\; \cdots \;\; U_{J_2}^n]^T$. Then,

$$U^n = AU^{n+1} + D^{n+1}.$$

Then, we obtain the following equation $U^n = AU^{n+1} + D^{n+1}$ for $n = N-1, \cdots, 2, 1$, with final condition $U_j^N = 0$ for $j = 1, 2, \cdots, J$.

4. Results: Numerical Simulation.

In practice, only the values of $V^\delta|_\Gamma$ are given by some experimental measures, and thus subject to experimental/measurement errors. In our examples, $V^\delta|_\Gamma$ is obtained by considering additive-multiplicative noise

$$V^\delta(t,x) = V(t,x) + (aV+b)\text{rand}_\Delta(t,x) \quad \text{for all } (t,x) \in \Gamma, \tag{21}$$

for scalars a, b, and rand_Δ is a uniformly distributed random variable taking values in the range $[-\Delta, \Delta]$. The threshold δ is such that (cf. Eq. (3)) $\|(aV+b)\text{rand}_\Delta\|_{L^2(\Gamma)} \leq \delta$, and we impose then

$$\|(aV+b)\|_{L^2(\Gamma)}\Delta = \delta. \tag{22}$$

In our numerical examples, we use multiplicative and additive noises, i.e., $a = 1/2$ and $b = 1/2$ at Eq. (21). We noticed no qualitative difference in the results for other values of a and b. In all Figures, we plot results for $\Delta = 1\%$ of noise.

We present four numerical tests. In the first three examples the geometry is defined by a segment, and in the fourth example is given by a tree. The first example considers only one ion (Ion $= \{\text{K}\}$), with $\boldsymbol{G}(x) = G_{\text{K}}(x)$ dependent only the spatial variable, and the voltage is known at $\Gamma = [0,T] \times \{0, L\}$, i.e., at all times but only at the end-points. In the second example, still with one ion (Ion $= \{\text{K}\}$), the conductance depends on the temporal and spatial variables (t,x) and measured voltage is known at $\Gamma = [0,T] \times [0,L]$, i.e., all the time and at all points. In the third example, we consider two ions (Ion $= \{\text{K}, \text{Na}\}$), where $\boldsymbol{G}(x) = (G_{\text{K}}(x), G_{\text{Na}}(x))$ depends only on the spatial variable and the data is again known at $\Gamma = [0,T] \times [0,L]$, i.e., all the time for all points. Finally, in the fourth example we consider the case where the geometry is defined by a tree, with the conductance being time independent under the presence of one ion, and the voltage data being known at all the time and all the points.

For all our numerical examples we consider the following values: $r_a = 0.0238$ (cm), $R = 34.5$ (Ωcm), $C_M = 1$ $(\Omega F/cm^2)$; $G_L = 0.3$ (mS/cm^2), $E_L = 10.613$ (mV), $T = 20$ (ms) and

$L = 0.1\ (cm)$. Also, we consider the following boundary and initial conditions,

$$V_x(t,0) = p(t) = -\frac{Rt^2 \exp(-10t)}{\pi {r_a}^2}; \quad V_x(t,L) = q(t) = 0; \quad V(0,x) = r(x) = 0$$

We solve equations (1) and (8) via finite differences in space, with $\Delta x = 0.001\ (cm)$, and in time, with $\Delta t = 0.2\ (ms)$, with the parameters and kinetics as specified above. For stopping criterion (6), we choose $\tau = 2.01$. Our initial guess is zero in all numerical tests, so the initial error is 100%. Finally, we consider $M = 100$ experiments.

Example 4.1. *Consider a particular instance from Eq.* (1)*, where* $N_{ion} = 1$ $(Ion = \{K\})$*,* $E_K = -12\ (mV)$ *and* $G_i(t,x) = G_K(x)$*. The goal is to estimate*

$$G_K(x) = 0.2 + 0.2/\left(\ 1 + \exp(\ (\ 0.1/2 - x\ )/0.01\ )\ \right)\ (mS/cm^2)$$

given $V^\delta|_\Gamma = \left\{V^\delta(t,0),\ V^\delta(t,0.1);\ t \in [0,20]\right\}$.

In Figures 3 and 4, we plot results for $\Delta = 5\%$ *of noise with* $M = 100$ *experiments. In Figure 3, we display the exact membrane potential, the mean and standard deviation its measurement, and difference between the exact membrane potential and mean of its measurements. In Figure 4, we show the exact conductance, the mean and standard deviation of the approximate solutions, and difference between the conductance and mean of the approximate solutions.*

Example 4.2. *We consider conductance as depending on time and space, where* $N_{ion} = 1$ $(Ion = \{K\})$*,* $E_K = -12\ (mV)$*,* $G_i(t,x) = G_K(t,x)$*. The goal is to estimate*

$$G_K(t,x) = 0.2 + 0.2/\left(\ 1 + \exp(\ (\ 0.1/2 - x\ )/0.01\ )\ \right) + t + 1\ (mS/cm^2)$$

given $V^\delta|_\Gamma = \left\{V^\delta(t,x);\ (t,x) \in [0,20] \times [0,0.1]\right\}$.

This example is harder than the previous one since now the conductance depends on both time and space. In Figures 5 and 6, we plot numerical results for $\Delta = 5\%$ *of noise with* M *experiments. Observe that the data for both* $V^\delta|_\Gamma$ *and* G_K *depend on time and space.*

Example 4.3. *Consider now two different ions, K and Na, where* $N_{ion} = 2$ $(Ion = \{K, Na\})$ $E_K = -12\ [mV]$ *and* $E_{Na} = 115\ [mV]$*. The goal is to approximate*

$$G_K(x) = 0.2 + 0.2/\left(\ 1 + \exp(\ (\ 0.1/2 - x\ )/0.01\ )\ \right)$$

and

$$G_{Na}(x) = 0.1 + 0.1/\left(\ 1 + \exp(\ (\ 0.1/2 - x\ )/0.01\ )\ \right),$$

given $V^\delta|_\Gamma = \left\{V^\delta(t,x);\ (t,x) \in [0,20] \times [0,0.1]\right\}$.

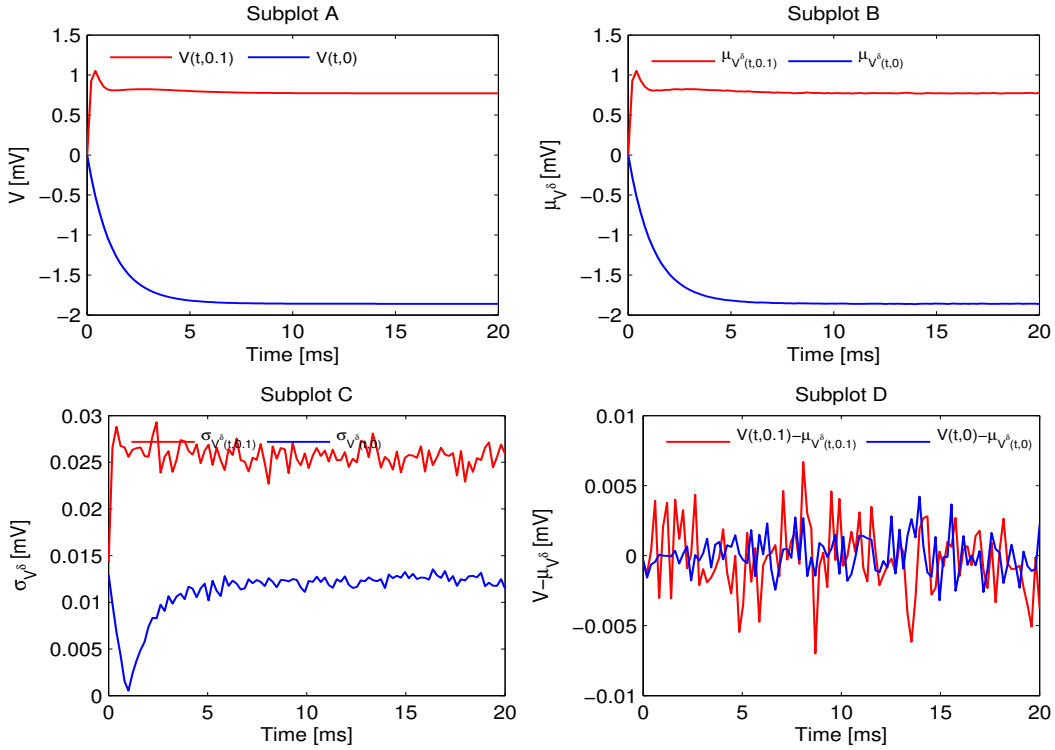

FIGURE 3. Result for Example 4.1 with $\Delta = 5\%$ noise. Subplot A presents the exact, deterministic, membrane potential at the end-points. Subplots B and C show the mean and standard deviation of the one hundred membrane potential measurements, respectively. In Subplot D displays the difference between the exact membrane potential and the mean of its measurements.

The extra difficulty in this lies in the fact that there are two conductance functions to be discovered. In Figures 7, 8 and 9, we plot results for $\Delta = 5\%$ of noise with M experiments. Note that now there are two conductances, one related to K and the other to Na.

Example 4.4. *As our final example, we consider the domain defined by a tree, as discussed in Section 1.1, in particular Eq.* (9). *We consider, $N_{ion} = 1$ ($Ion = \{K\}$), $E_K = -12$ (mV) and $G_i(t,x) = G_K(x)$. The length of the edges are: $|e_1| = |e_2| = 0.1$ (cm) and $|e_3| = 0.2$ (cm), in addition vertex $\nu_1 = 0$. The values of the other parameters are the same. In this case, We solve the differential equations* (9) *and* (10) *through finite differences (Euler Explicit) with $\Delta x = \Delta t = 0.01$.*

The goal of this example, given $V^\delta(t,x)$ in all $(t,x) \in (0,T) \times \Theta$, is to estimate

$$G_K(x) = \begin{cases} 0.2 + 0.2/\,(\,1 + \exp(\,(\,0.1/2 - \mathrm{dist}(x,\nu_1)\,)/0.01\,)\,) & \text{if } x \in e_1, \\ 0.2 + 0.2/\,(\,1 + \exp(\,(\,0.1/2 - 0.01 - \mathrm{dist}(x,\nu_2)\,)/0.01\,)\,) & \text{if } x \in e_2 \cup e_3, \end{cases}$$

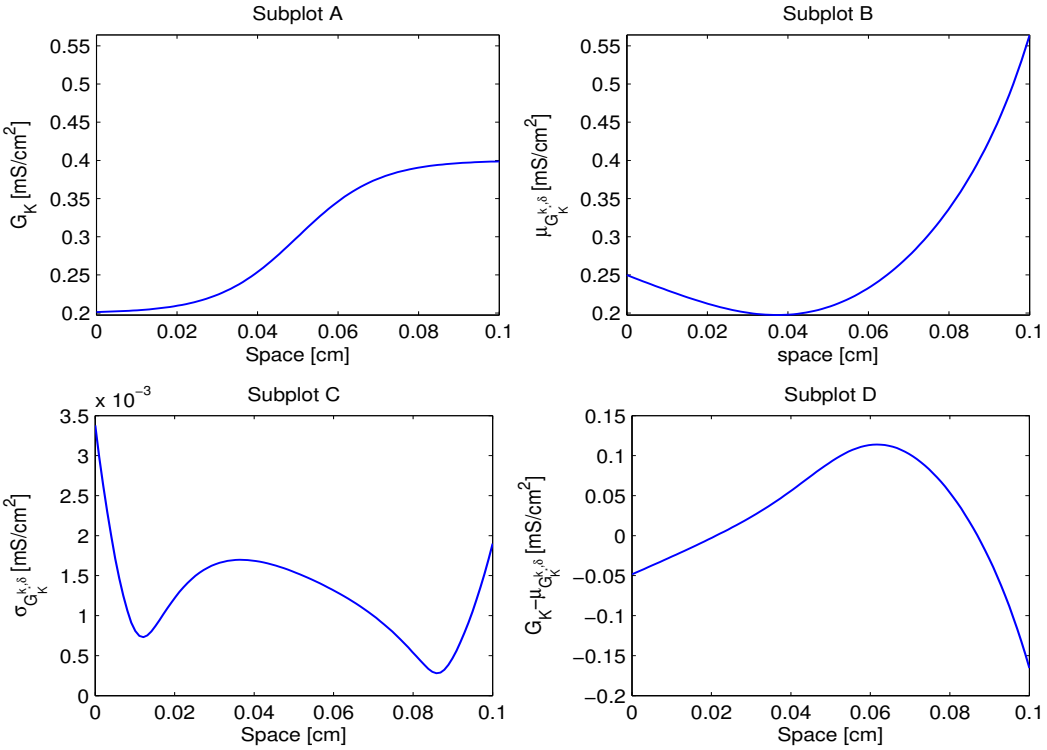

FIGURE 4. For Example 4.1 with $\Delta = 5\%$. Subplot A shows the exact solution G_{K}. In subplots B and C present the mean and standard deviation of the one hundred approximate solutions, respectively. Subplot D displays the difference between the exact solution and mean of the approximate solutions.

where $\mathrm{dist}(a, b)$ *denotes the distance between the points* a *and* b*. In figures 10–15, we plot numerical result for* $\Delta = 5\%$*.*

REFERENCES

[1] VALLE, J. A. M., MADUREIRA, A. L., AND LEITÃO, A. A computational approach for the inverse problem of neuronal conductances determination. *arXiv preprint arXiv:1810.05887* (2018).

DEPARTAMENTO DE MODELAGEM COMPUTACIONAL, LABORATRIO NACIONAL DE COMPUTAO CIENTFICA, AV. GETLIO VARGAS 333, 25651-070 PETRPOLIS, RJ, BRAZIL

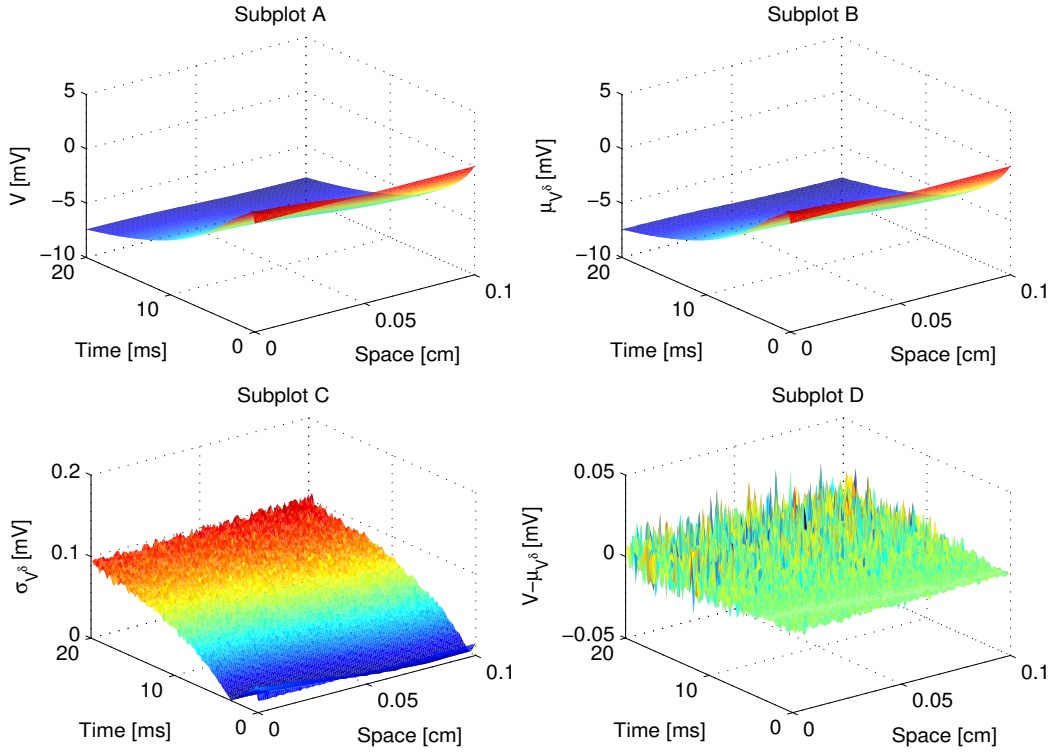

FIGURE 5. Result for Example 4.2 with $\Delta = 5\%$ noise. See Figure 3 for the subplots description.

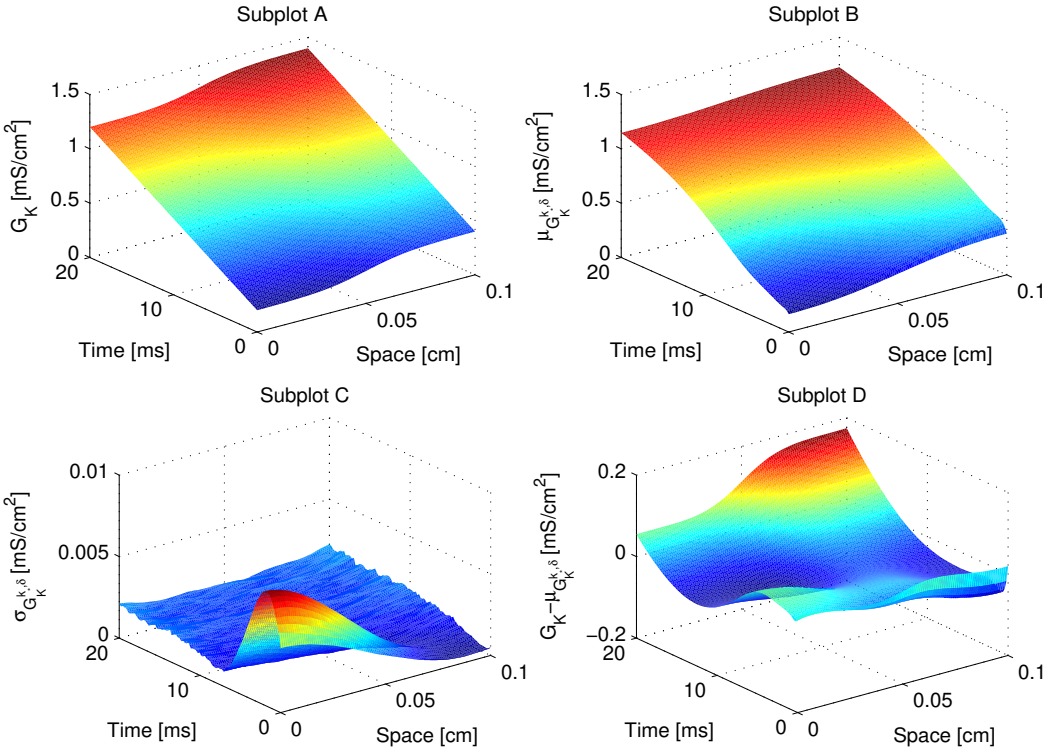

FIGURE 6. For Example 4.2 with $\Delta = 5\%$. Subplot A shows the exact solution G_{K}. See Figure 4 for the subplots description

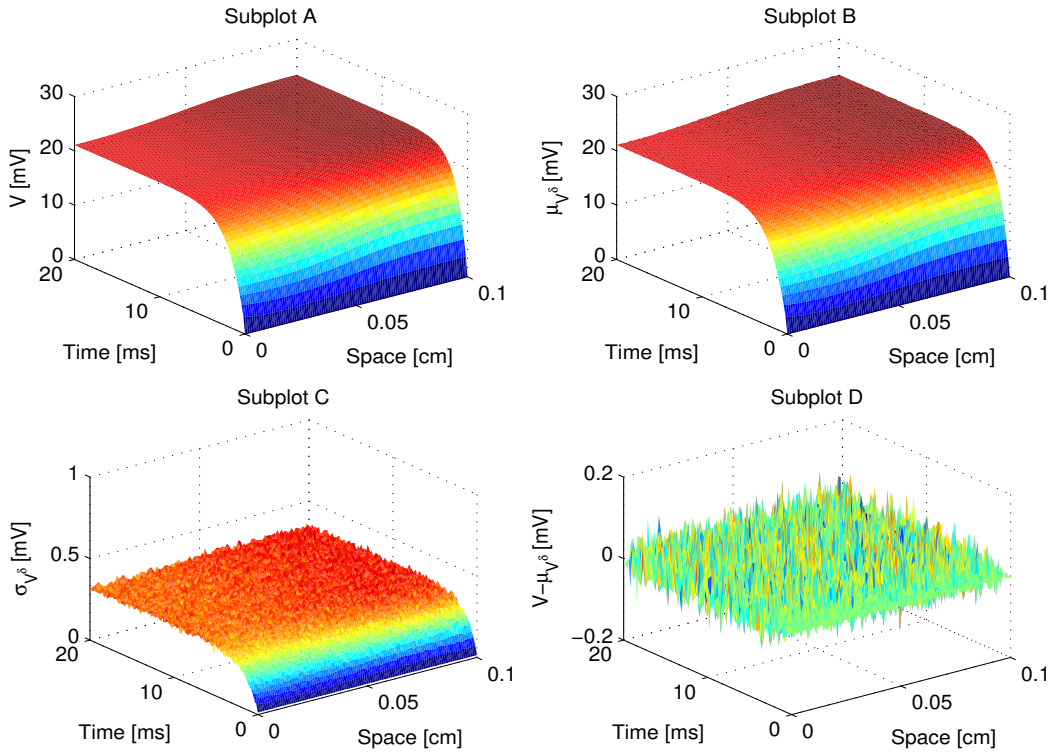

FIGURE 7. Result for Example 4.3 with $\Delta = 5\%$ noise. See Figure 3 for the subplots description.

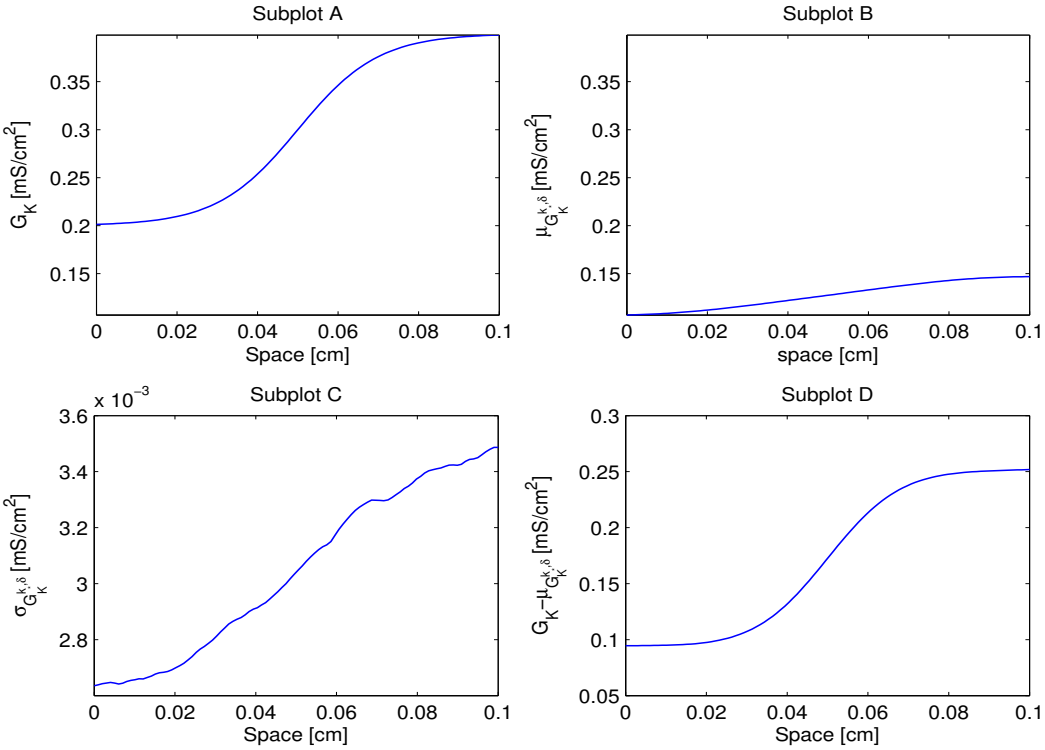

FIGURE 8. For Example 4.3 with $\Delta = 5\%$. See Figure 4 for the subplots description

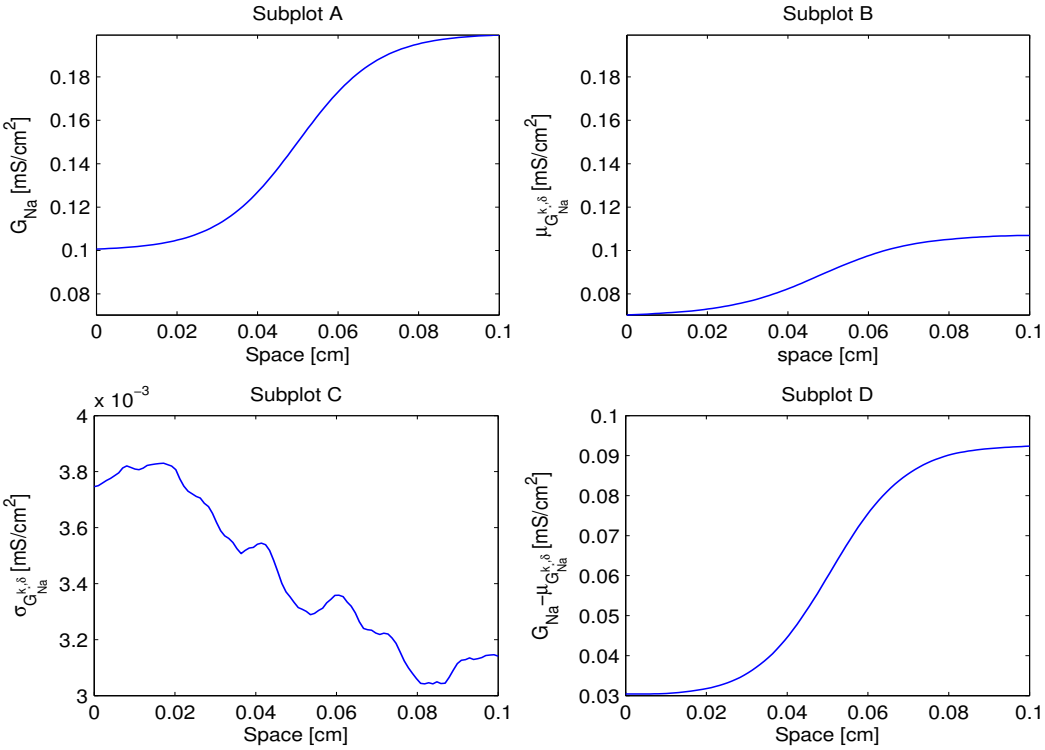

FIGURE 9. For Example 4.3 with $\Delta = 5\%$. See Figure 4 for the subplots description

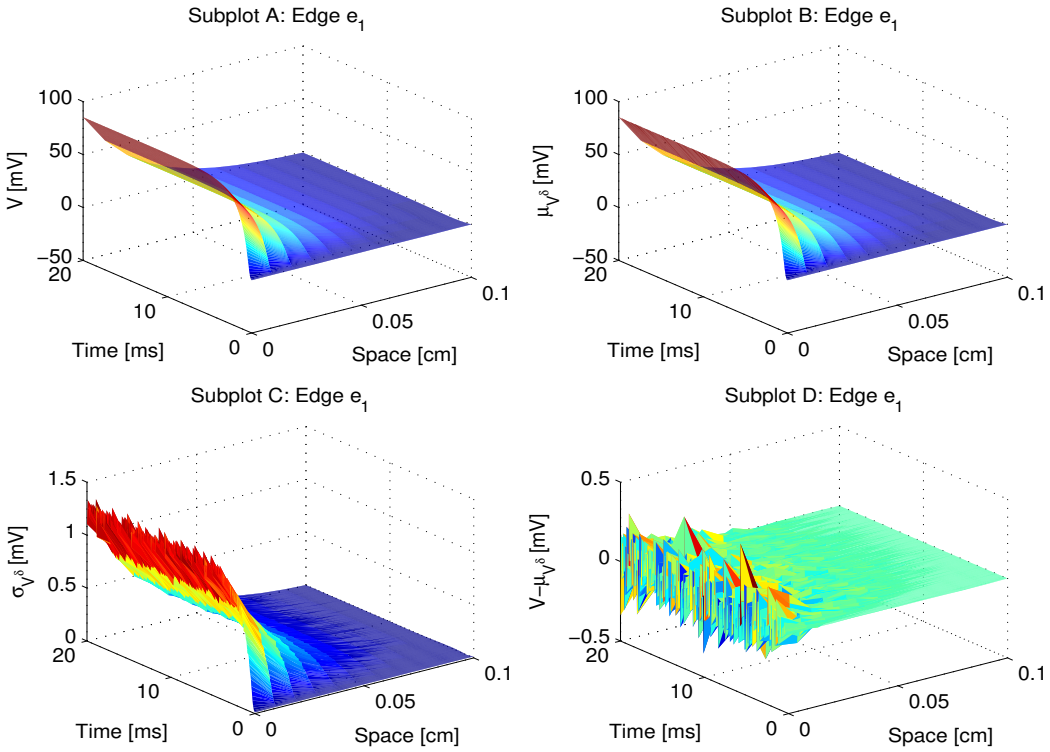

FIGURE 10. For Example 4.4 and edge e_1, with $\Delta = 5\%$. See Figure 3 for the subplots description.

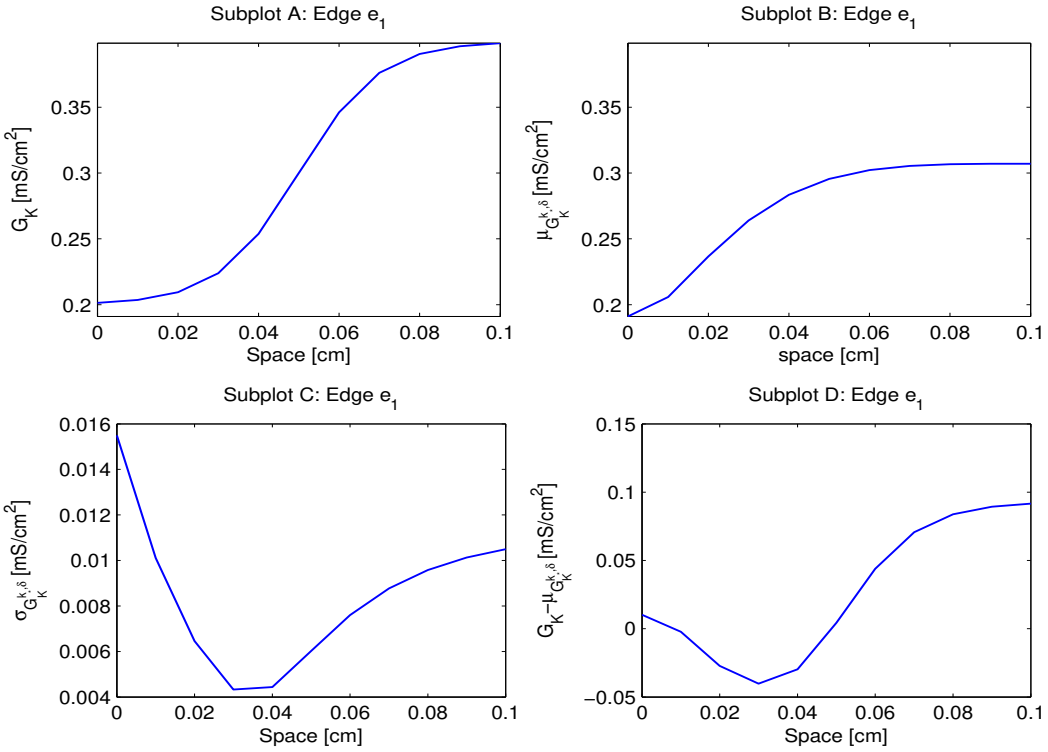

FIGURE 11. Plots for Example 4.4 and edge e_1. See Figure 4 for the subplots description.

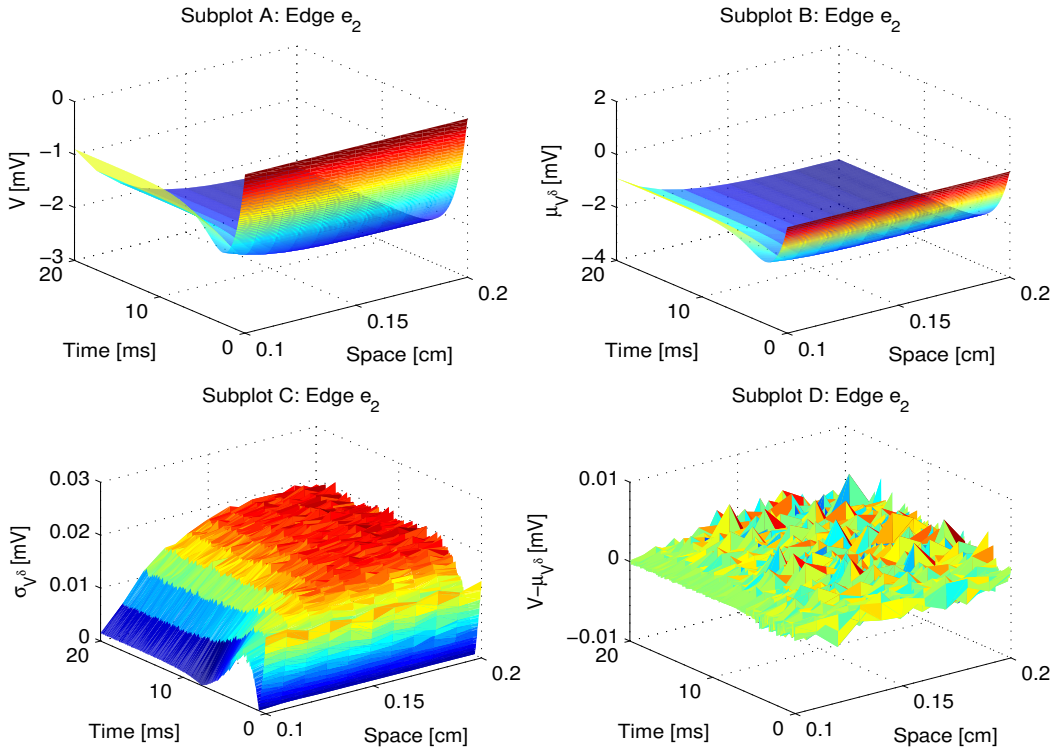

FIGURE 12. For Example 4.4 and edge e_2, with $\Delta = 5\%$. See Figure 3 for the subplots description.

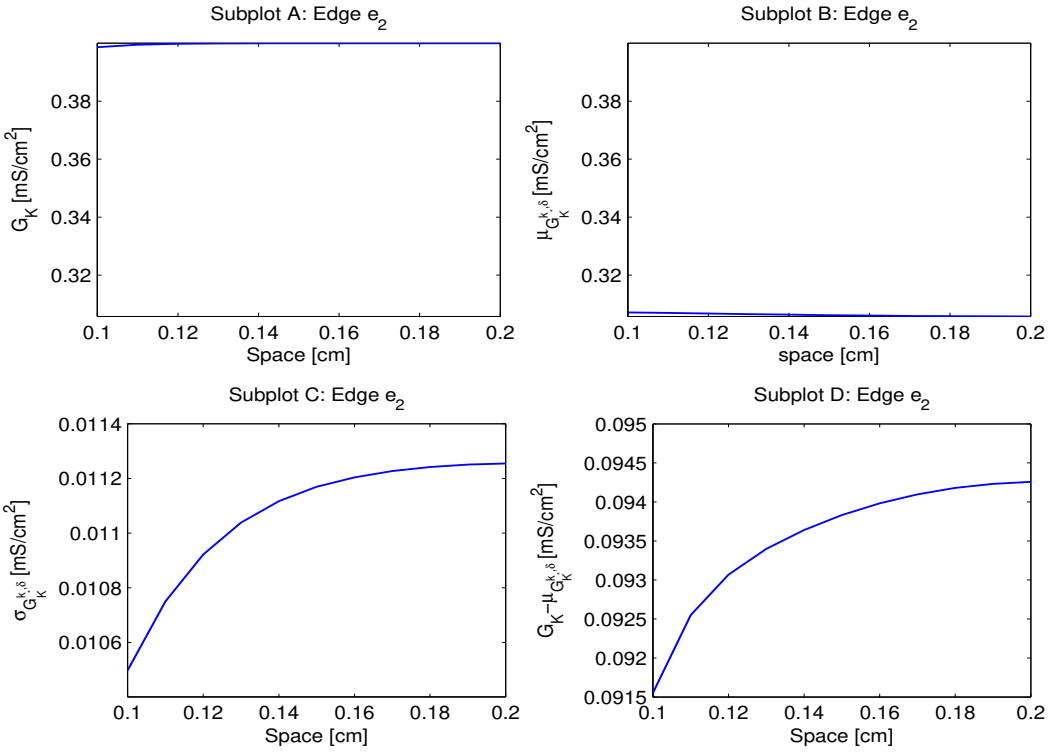

FIGURE 13. Plots for Example 4.4 and edge e_2. See Figure 4 for the subplots description.

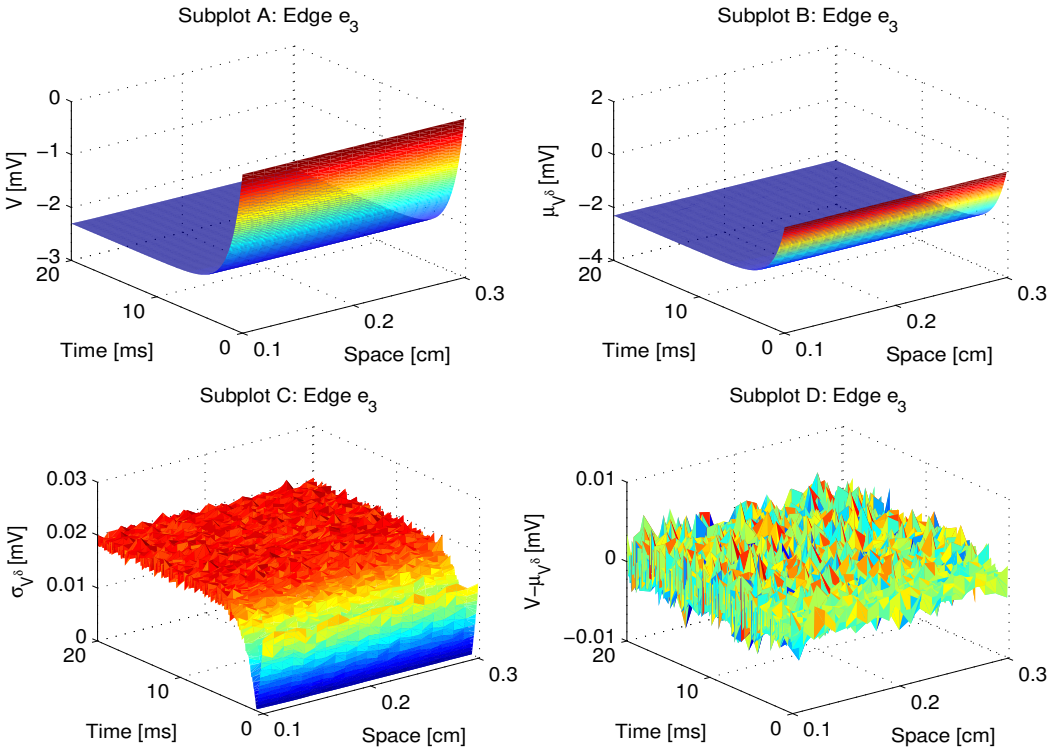

FIGURE 14. For Example 4.4 and edge e_3, with $\Delta = 5\%$. See Figure 3 for the subplots description.

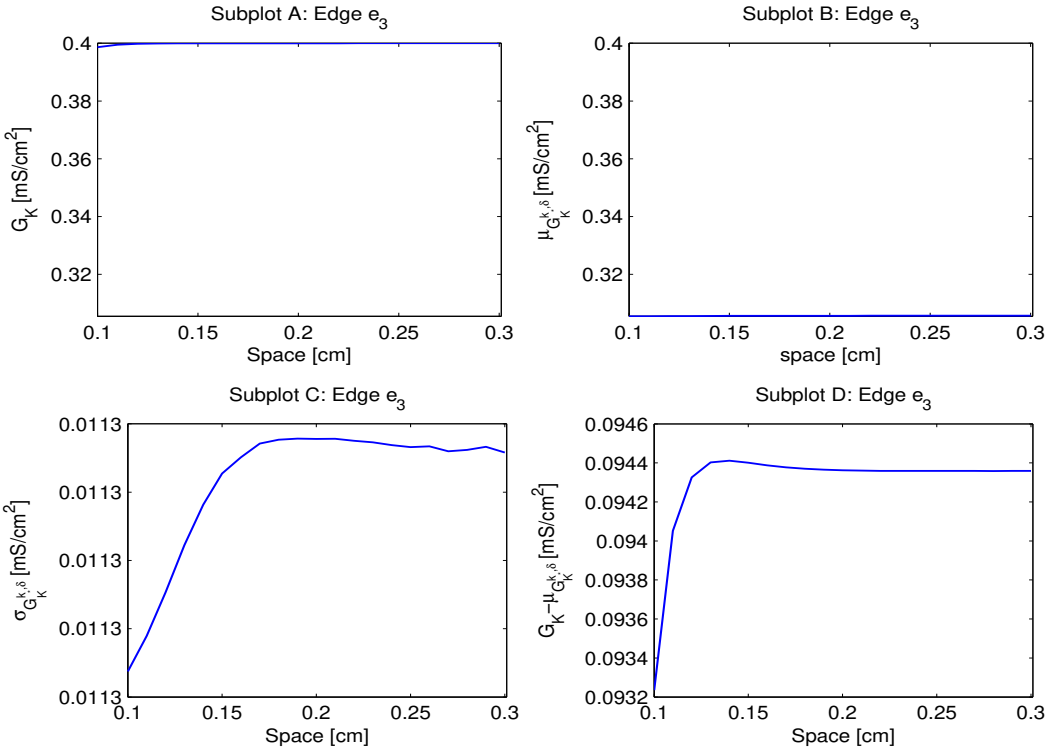

FIGURE 15. Plots for Example 4.4 and edge e_3. See Figure 4 for the subplots description.